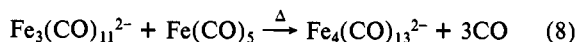


reaction is likely in view of the fact that  $\text{Fe}(\text{CO})_5$  reacts with  $\text{Fe}_3(\text{CO})_{11}^{2-}$  at elevated temperatures to produce  $\text{Fe}_4(\text{CO})_{13}^{2-}$ .<sup>22</sup>



Dissociation of CO from  $\text{Fe}(\text{CO})_5$  is known to occur readily at high temperatures, so the thermal reaction probably also proceeds by attack of an  $\text{Fe}(\text{CO})_n$  ( $n = 3$  or  $4$ ) fragment on  $\text{Fe}_3(\text{CO})_{11}^{2-}$ . Evidence that Fe—CO dissociation is still the primary photoprocess in  $\text{CH}_2\text{Cl}_2$  solution is our observation that 1 atm of CO inhibits the photoreaction.

(22) Hieber, W.; Schubert, E. H. *Z. Anorg. Allg. Chem.* 1965, 338, 37.

The aqueous solution photochemistry of  $\text{Fe}_3(\text{CO})_{11}^{2-}$  is readily understood in terms of either of the pathways outlined in Scheme II. Direct fragmentation of the  $\text{Fe}_3(\text{CO})_{11}^{2-}$  cluster could occur at the relatively high excitation energies involved (pathway A). Pathway B is similar to the mechanism in Scheme I in that Fe—CO dissociation is the primary photoprocess. Note that two Fe(0) fragments are formed along either pathway. In the absence of trapping agents these fragments are expected to be unstable with respect to oxidation; such redox decomposition gives two molecules of  $\text{Fe}(\text{OH})_2$  and two molecules of  $\text{H}_2$ .

**Acknowledgment.** This research was supported by National Science Foundation Grant No. CHE78-10530.

## Electronic Spectra of Copper(II)–Imidazole and Copper(II)–Pyrazole Chromophores

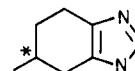
Ernest Bernarducci, William F. Schwindinger, Joseph L. Hughey, IV, Karsten Krogh-Jespersen, and Harvey J. Schugar\*

Contribution from the Department of Chemistry, Rutgers—The State University of New Jersey, New Brunswick, New Jersey 08903. Received August 11, 1980

**Abstract:** Solution spectra covering the 50 000–20 000- $\text{cm}^{-1}$  region are reported for tetrakis complexes of Cu(II) with various imidazole and pyrazole ligands. Such complexes exhibit three ligand to metal charge-transfer (LMCT) absorptions, which originate from the  $\text{sp}^2$ -type nitrogen lone pair ( $n$ ) and from two  $\pi$ -symmetry ring orbitals, one (HOMO,  $\pi_1$ ) with mostly carbon character and the other ( $\pi_2$ ) with substantial nitrogen character. The  $\pi$ -symmetry absorptions are relatively weak and poorly resolved for solutions containing tetrakis complexes of Cu(II) with either unsubstituted imidazole or pyrazole. Alkylation of either type of ligand causes the  $\pi$ -symmetry absorptions to be prominent well-resolved features of the solution spectra. Tetragonal Cu(II) complexes containing alkylated ligands of either type exhibit absorptions at approximately 46 000  $\text{cm}^{-1}$  (ligand  $\pi \rightarrow \pi^*$  and  $n(\text{ligand}) \rightarrow \text{Cu}(\text{II})$  LMCT), 33 000  $\text{cm}^{-1}$  ( $\pi_2(\text{ligand}) \rightarrow \text{Cu}(\text{II})$  LMCT), 29 000  $\text{cm}^{-1}$  ( $\pi_1(\text{ligand}) \rightarrow \text{Cu}(\text{II})$  LMCT), and 16 000  $\text{cm}^{-1}$  (ligand field transitions). The electronic structures, ligand  $\pi \rightarrow \pi^*$  absorptions, and ligand  $n \rightarrow \text{Cu}(\text{II})$  LMCT absorptions are very similar for imidazoles and pyrazoles. Published LMCT spectra of various pyrazolylborate- and pyrazolylgallate-Cu(II) complexes have been reassigned from the above point of view. The LMCT absorptions exhibited by a pseudotetrahedral Cu(II) complex of this type are red shifted by 10 000–12 000  $\text{cm}^{-1}$  relative to planar Cu(II) reference complexes. Analogous absorptions in the visible–near-UV spectra of type I copper proteins are thought to result from Cu(II)–imidazole ligation. Finally, circular dichroism spectra are presented of solutions containing Cu(II) and (+)-5-methyl-4,5,6,7-tetrahydrobenzimidazole.

In a previous paper we have characterized the ligand to metal charge-transfer (LMCT) absorptions of several model Cu(II)–imidazole (ImH) complexes.<sup>1</sup> These transitions originate from the three highest lying imidazole orbitals, i.e., the  $\sigma$ -symmetry nitrogen donor lone pair ( $n$ ) and two  $\pi$ -symmetry ring orbitals ( $\pi_1$ ,  $\pi_2$ ). The solid-state spectra of tetragonal Cu(II)–ImH chromophores exhibit prominent  $n(\text{ImH}) \rightarrow \pi_2(\text{ImH}) \rightarrow$ , and  $\pi_1(\text{ImH}) \rightarrow \text{Cu}(\text{II})$  LMCT absorptions at  $\sim 220$ ,  $\sim 260$ , and  $\sim 330$  nm, respectively; the  $\pi \rightarrow \pi^*$  absorption of free and complexed ImH appears at  $\sim 205$  nm. The  $\pi \rightarrow \text{M}$  bands were not well-resolved features in the solution spectra of the same complexes, in contrast to the  $\sigma \rightarrow \text{M}$  bands. We interpreted the broadening of the  $\pi \rightarrow \text{M}$  bands as indicating that the Cu(II)–ImH units of the solution complexes adopt a range of conformations around the Cu–N axis. The  $\sigma \rightarrow \text{M}$  absorption should be rather insensitive to such rotations. We report here an extension of these studies to Cu(II) complexes of 4,5-disubstituted imidazoles such as 4,5-diisopropylimidazole, 4,5-diethylimidazole, and 4,5,6,7-tetrahydrobenzimidazole. Solution spectra of these complexes exhibit well-resolved  $\pi_2(\text{ImH}) \rightarrow \text{Cu}(\text{II})$  and  $\pi_1(\text{ImH}) \rightarrow \text{Cu}(\text{II})$  bands. We also report preliminary circular dichroism

spectra for the Cu(II) complex of (+)-5-methyl-4,5,6,7-tetrahydrobenzimidazole.



Finally, we present an analysis of the LMCT spectra of Cu(II)–pyrazole (Pz) complexes. The electronic structures of ImH and Pz are very similar, and we show that the LMCT spectra of Cu(II)–Pz complexes mirror those of Cu(II)–ImH complexes and also have considerable bioinorganic relevance. In particular, the LMCT spectra of an approximately tetrahedral Cu(II)–Pz chromophore allow the convincing prediction that analogous low energy absorptions are to be expected from the Cu(II)–ImH units in the type I copper proteins.<sup>2</sup>

### Experimental Section

**Preparation of 4,5-Diethylimidazole.** Propionoin was prepared by the acyloin condensation<sup>3</sup> of ethyl propionate and converted to 4,5-diethylimidazole by reaction with refluxing formamide.<sup>4</sup> After removal of the

(1) Fawcett, T. G.; Bernarducci, E. E.; Krogh-Jespersen, K.; Schugar, H. *J. Am. Chem. Soc.* 1980, 102, 2598–2604.

(2) Solomon, E. I.; Hare, J. W.; Dooley, D. M.; Dawson, J. H.; Stephens, P. J.; Gray, H. B. *J. Am. Chem. Soc.* 1980, 102, 168–178.

(3) Snell, J. M.; McElvain, S. M. "Organic Syntheses"; Wiley: New York, 1943; Collected Vol. II, pp 114–115.

Table I. Comparison of the Ionization Potentials (eV) of Imidazole and Pyrazole<sup>a</sup>

orbitals <sup>b</sup>			method	ref
$\pi_1$	$\pi_2$	n		
9.87 (10.49)	11.51 (10.87)	11.62 (11.99)	CNDO/S	9
9.19 (9.81)	11.09 (10.41)	11.77 (12.50)	ab initio	10
10.6 (11.1)	12.3 (11.7)	12.7 (13.4)	ab initio	11
8.92 (9.04)	10.15 (10.39)	10.25 (11.06)	ab initio <sup>c</sup>	12
8.78 (9.15)	10.3 (9.88)	10.3 (10.7)	exptl (PES)	12

<sup>a</sup> IP's for pyrazole are given in parentheses. <sup>b</sup> See Figure 1 and text for definitions of the ligand orbitals. <sup>c</sup> The IP's shown here include a scaling factor of 0.799 recommended by the authors of ref 12.

excess formamide by distillation, the product was obtained as a fraction which boiled at 120–125 °C (~1 mm) (lit.,<sup>4</sup> 150–160 °C (10 mm)). An occasional application of a heat lamp was required to prevent the product from solidifying in the air-cooled condenser. After several recrystallizations from mixtures of deionized water and spectrograde ethanol, the white crystalline product melted at 79–82 °C (lit.,<sup>4</sup> 82–85 °C); <sup>1</sup>H NMR (CDCl<sub>3</sub>, 60 MHz)  $\delta$  1.4 (t,  $J$  = 8 Hz, 6 H, CH<sub>3</sub>), 2.6 (q,  $J$  = 8 Hz, 4 H, CH<sub>2</sub>), 7.5 (s, 1 H, ArH), 11.5 (s, 1 H, NH).

**Preparation of 4,5-Diisopropylimidazole.** Isobutyroin was prepared by the acyloin condensation<sup>3</sup> of methyl isobutyrate and converted to the imidazole by reaction with refluxing formamide.<sup>4</sup> The formate salt of the product separated as white crystals when the reaction mixture was cooled to room temperature. The free ligand precipitated as a white solid when an aqueous solution of the formate salt was neutralized with aqueous NH<sub>3</sub>. After several recrystallizations from mixtures of deionized water and spectrograde ethanol, the white crystalline product melted at 200–202 °C (lit.,<sup>4</sup> 214 °C); <sup>1</sup>H NMR (CDCl<sub>3</sub>, 60 MHz)  $\delta$  1.3 (d,  $J$  = 6 Hz, 12 H, CH<sub>3</sub>), 3.1 (m, 2 H, CH), 7.6 (s, 1 H, ArH), 8.6 (s, 1 H, NH).

**Preparation of 4,5,6,7-Tetrahydrobenzimidazole.** Adipoin was prepared by the acyloin condensation<sup>5</sup> of adipic acid dimethyl ester and reacted with an alkaline Cu(II) acetate-formalin mixture.<sup>6</sup> The resulting Cu(I) complex of the tetrahydrobenzimidazole was decomposed with aqueous Na<sub>2</sub>S and the precipitated Cu<sub>2</sub>S removed by filtration. The free ligand crystallized from the cooled filtrate as white crystals in 30% yield (based on adipoin). After several recrystallizations from deionized water, the free ligand melted at 145 °C (lit.,<sup>6</sup> 152 °C); <sup>1</sup>H NMR (CDCl<sub>3</sub>, 60 MHz)  $\delta$  1.9 (m, 4 H, CH<sub>2</sub>), 2.7 (m, 4 H, CH<sub>2</sub>), 7.6 (s, 1 H, ArH), 12 (s, 1 H, NH).

**Preparation of (+)-5-Methyl-4,5,6,7-tetrahydrobenzimidazole.** Following a published procedure,<sup>7</sup> we prepared the required diester by azeotropic water removal from a mixture of (+)-3-methyladipic acid (Aldrich Chemical Co.), toluene, absolute ethanol, and H<sub>2</sub>SO<sub>4</sub>. The diester was isolated by distilling the residue at reduced pressure (water aspirator). The colorless diester was obtained as the 147–152 °C fraction (97% yield from diacid). The presence of the desired methyladipoin in the crude product obtained from the acyloin<sup>5</sup> condensation of the diester was consistent with the infrared absorption at 3480 cm<sup>-1</sup> and <sup>1</sup>H NMR spectra. The crude product was reacted with alkaline Cu(II) acetate and formalin,<sup>6</sup> and the poorly soluble Cu(II) salt of the product imidazole was isolated by filtration and washed with ethanol and water.<sup>8</sup> The free ligand was isolated as described above. After several recrystallizations from deionized water, the white crystalline product melted at 121–122 °C; <sup>1</sup>H NMR (CDCl<sub>3</sub>, 60 MHz)  $\delta$  1.05 (d,  $J$  = 4 Hz, 3 H, CH<sub>3</sub>), 2 (complex m, 3 H, CH, CH<sub>2</sub>), 2.8 (complex m, 4 H, CH<sub>2</sub>), 7.5 (s, 1 H, ArH), 8 (s, 1 H, NH). The yield of recrystallized product was 10% based upon the diester.

**Pyrazoles.** Both pyrazole and 3,5-dimethylpyrazole were obtained from the Aldrich Chemical Co. The 3,5-dimethylpyrazole was recrystallized three times from a mixture of spectrograde ethanol and deionized water. The pyrazole was used as received; extraneous UV absorptions were not observed in the commercial product.

**Physical Measurements.** Electronic spectra were recorded on a Cary Model 17 that was interfaced with a Tektronix computer. Circular dichroism spectra were recorded on a Cary Model 61 instrument.

(4) Bredereck, H.; Theilig, G. *Chem. Ber.* **1953**, *86*, 88–93.

(5) Sheehan, J. C.; O'Neill, R. C.; White, M. A. *J. Am. Chem. Soc.* **1950**, *72*, 3376–3378.

(6) Weidenhagen, R.; Wegner, H. *Chem. Ber.* **1938**, *71*, 2124–2134.

(7) Vogel, A. I. "Practical Organic Chemistry", 3rd ed.; Longman: London, 1974; pp 385–386.

(8) Apparently the byproducts of the acyloin condensation do not interfere with the production of the Cu(I) salt and readily may be separated from it.

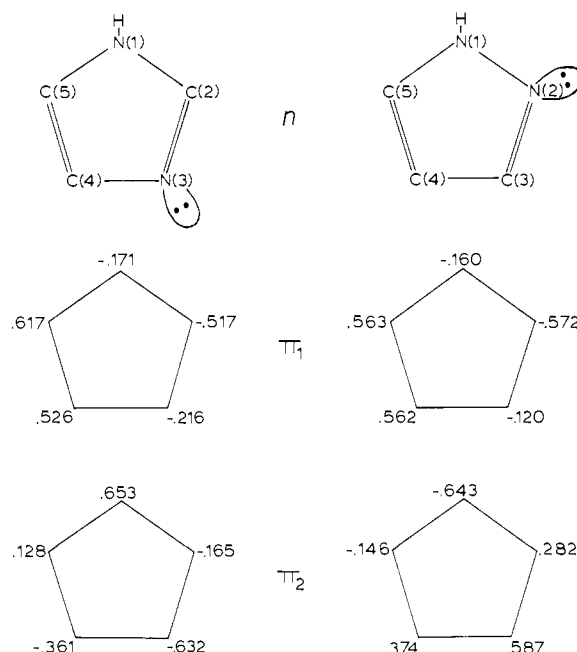


Figure 1. Numbering schemes for ImH and Pz along with the MO coefficients of Del Bene and Jaffé.<sup>9</sup>

## Results and Discussion

**Electronic Structures of Imidazole and Pyrazole.** The electronic structure of free ImH, although described previously in detail,<sup>1</sup> is briefly reconsidered here for comparison with that of free Pz. Spectroscopically relevant calculated<sup>9–12</sup> and measured<sup>12</sup> ionization potentials are summarized in Table I; only studies which have presented comparisons between ImH and Pz at the same calculational levels have been considered here. All of these calculations yield the result that both ImH and Pz possess three occupied molecular orbitals (MO's) of relatively high energy, which are well removed (>3 eV) from the lower lying corelike orbitals. The two highest lying orbitals are of  $\pi$  symmetry ( $\pi_1$ ,  $\pi_2$ ) and the third orbital represents the lone pair ( $\sigma$  symmetry) on the pyridine-type nitrogen atom (n). The calculations clearly indicate an increase in the first ionization potential on going from ImH to Pz, accompanied by a decrease in the  $\pi_1$ – $\pi_2$  and an increase in the  $\pi_2$ –n orbital energy separations. Experimental support for these results comes from the published gas-phase photoelectron spectra<sup>12</sup> of the free ligands. Transitions at 8.78 and 9.15 eV reasonably have been assigned to ionization from the  $\pi_1$  levels of ImH and Pz, respectively. Ionization from approximately degenerate  $\pi_2$  and n levels of ImH yields a broad transition centered at 10.3 eV, whereas the corresponding processes in Pz give rise to well-resolved transitions at 9.88 and 10.7 eV, respectively.

Views of ImH and Pz along with the MO coefficients of  $\pi_1$  and  $\pi_2$  reported by Del Bene and Jaffé<sup>9</sup> are shown in Figure 1. The MO coefficients are very similar in the two molecules for both  $\pi_1$  and  $\pi_2$ . The HOMO of ImH ( $\pi_1$ ) has almost exclusively carbon character, while  $\pi_2$  is composed primarily of nitrogen 2p( $\pi$ ) orbitals. The interchange of ImH (C(2), N(3)) to Pz (N(2), C(3)) gives  $\pi_1$  more nitrogen and  $\pi_2$  less nitrogen character in Pz relative to ImH. Consideration of these coefficients and the larger nuclear attraction of nitrogen over carbon provides a simple rationalization of the movements in the  $\pi_1$  and  $\pi_2$  IP's associated with the above interchange.

The first observable electronic absorption band of free ImH is a  $\pi \rightarrow \pi^*$  transition.<sup>13</sup> Our spectral studies of ImH ligands reveal that the  $\pi \rightarrow \pi^*$  absorption in free ImH (48 500 cm<sup>-1</sup>,  $\epsilon$

(9) Del Bene, J.; Jaffé, H. H. *J. Chem. Phys.* **1968**, *48*, 4050–4055.

(10) Ha, T. K. *J. Mol. Struct.* **1979**, *51*, 87–98.

(11) Popkie, H. E.; Kaufman, J. J. *J. Chem. Phys.* **1977**, *66*, 4827–4831.

(12) Craddock, S.; Findlay, R. H.; Palmer, M. H. *Tetrahedron* **1973**, *29*, 2173–2181.

(13) Grebow, P. E.; Hooker, T. M., Jr. *Biopolymers* **1975**, *14*, 871–881.

**Table II.** Summary of Spectral Results and Assignments for Cu(II)-Imidazole Systems

system <sup>a</sup>	$\bar{\nu}$ , cm <sup>-1</sup>	$\epsilon^b$	assgnmnt
imidazole	48 500	6900	$\pi \rightarrow \pi^*$
4:1 imidazole:Cu(II)	48 800	41000	$\pi \rightarrow \pi^* + n(\text{ImH}) \rightarrow \text{Cu(II)}$
	32 300	340	$\pi_2(\text{ImH}) \rightarrow \text{Cu(II)} + \pi_1(\text{ImH}) \rightarrow \text{Cu(II)}$
	16 100	49	LF
8:1 imidazole:Cu(II)	32 300	370	$\pi_2(\text{ImH}) \rightarrow \text{Cu(II)} + \pi_1(\text{ImH}) \rightarrow \text{Cu(II)}$
	16 800	57	LF
4,5-diethylimidazole	45 500	8000	$\pi \rightarrow \pi^*$
4:1 4,5-diethylimidazole:Cu(II)	45 200	41000	$\pi \rightarrow \pi^* + n(\text{ImH}) \rightarrow \text{Cu(II)}$
	33 000	1770	$\pi_2(\text{ImH}) \rightarrow \text{Cu(II)}$
	29 000	1550	$\pi_1(\text{ImH}) \rightarrow \text{Cu(II)}$
	16 100	67	LF
8:1 4,5-diethylimidazole:Cu(II)	33 100	2110	$\pi_2(\text{ImH}) \rightarrow \text{Cu(II)}$
	28 700	1830	$\pi_1(\text{ImH}) \rightarrow \text{Cu(II)}$
	16 300	72	LF
4,5-diisopropylimidazole	45 600	6000	$\pi \rightarrow \pi^*$
4:1 4,5-diisopropylimidazole:Cu(II)	45 000	26800	$\pi \rightarrow \pi^* + n(\text{ImH}) \rightarrow \text{Cu(II)}$
	32 500	1640	$\pi_2(\text{ImH}) \rightarrow \text{Cu(II)}$
	28 600	1370	$\pi_1(\text{ImH}) \rightarrow \text{Cu(II)}$
	16 300	51	LF
4,5,6,7-tetrahydrobenzimidazole	45 200	7000	$\pi \rightarrow \pi^*$
4:1 4,5,6,7-tetrahydrobenzimidazole:Cu(II)	45 000	31000	$\pi \rightarrow \pi^* + n(\text{ImH}) \rightarrow \text{Cu(II)}$
	32 800	1790	$\pi_2(\text{ImH}) \rightarrow \text{Cu(II)}$
	28 800	1840	$\pi_1(\text{ImH}) \rightarrow \text{Cu(II)}$
	16 400	82	LF
(+)-5-methyl-4,5,6,7-tetrahydrobenzimidazole	45 200	6300	$\pi \rightarrow \pi^*$
4:1 (+)-5-methyl-4,5,6,7-tetrahydrobenzimidazole:Cu(II)	45 100	25700	$\pi \rightarrow \pi^* + n(\text{ImH}) \rightarrow \text{Cu(II)}$
	32 500	1600	$\pi_2(\text{ImH}) \rightarrow \text{Cu(II)}$
	28 700	1630	$\pi_1(\text{ImH}) \rightarrow \text{Cu(II)}$
	16 500	72	LF

<sup>a</sup> Spectra reported here were measured in CH<sub>3</sub>OH at 25 °C. Free ligands were 0.014 M; copper-containing systems were 0.0035 M in Cu(ClO<sub>4</sub>)<sub>2</sub>·6H<sub>2</sub>O and had ligand:Cu(II) ratios as indicated.

<sup>b</sup> Calculated per copper or per ligand in the copper-free systems.

6900) undergoes approximately a 3000-cm<sup>-1</sup> red shift when 4,5-dialkyl substitution is introduced (Table II). The  $\pi \rightarrow \pi^*$  transitions for 4,5-diethylimidazole, 4,5-diisopropylimidazole, 4,5,6,7-tetrahydrobenzimidazole, and (+)-5-methyl-4,5,6,7-tetrahydrobenzimidazole occur at 45 500 ( $\epsilon$  8000), 45 600 ( $\epsilon$  6000), 45 200 ( $\epsilon$  7000), and 45 000 cm<sup>-1</sup> ( $\epsilon$  7000), respectively. The close electronic structural kinship of Pz is reflected in an analogous  $\pi \rightarrow \pi^*$  transition (Table III) at 48 100 cm<sup>-1</sup> ( $\epsilon$  6300). Alkylation in the 3,5-positions causes a red shift of this transition to 46 700 cm<sup>-1</sup> ( $\epsilon$  5700). Other workers have published a detailed study of red shifts induced in the Pz  $\pi \rightarrow \pi^*$  transition by alkylation in the 3,4, and 5-positions.<sup>14</sup>

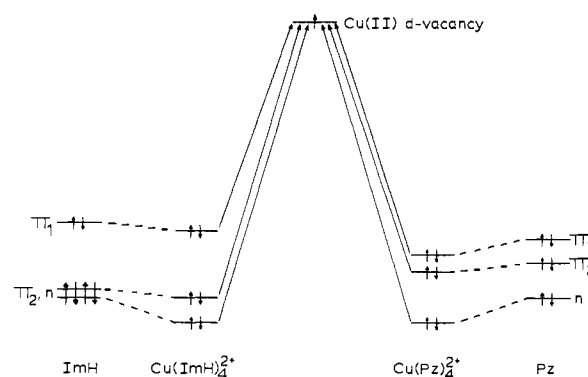
#### Electronic Spectra of Cu(II)-ImH and Cu(II)-Pz Complexes.

A qualitative MO diagram shown in Figure 2 indicates the essential electronic structural features of Cu(II)-ImH and Cu(II)-Pz units. In both units, the upper occupied ligand orbitals should be stabilized by the complexation. Considering the relative overlap between the Cu(II) and the ligand orbitals and the composition of the latter (Figure 1), the relative stabilization of the ligand orbitals is expected to be  $n \gg \pi_2 > \pi_1$  for the Cu(II)-ImH unit and  $n \gg \pi_1 > \pi_2$  for the Cu(II)-Pz units. Thus for both types of complexes the highest energy LMCT absorption should correspond to the  $n(\text{ImH}) \rightarrow \text{Cu(II)}$  and  $n(\text{Pz}) \rightarrow \text{Cu(II)}$  transitions. Since these transitions essentially have  $\sigma\text{-}\sigma^*$  character, they are expected to be relatively intense. Moreover, two somewhat weaker and red-shifted  $\pi$ -symmetry LMCT transitions are expected for

**Table III.** Summary of Spectral Results and Assignments for Cu(II)-Pyrazole Systems

system <sup>a</sup>	$\bar{\nu}$ , cm <sup>-1</sup>	$\epsilon^b$	assgnmnt
pyrazole	48 100	6300	$\pi \rightarrow \pi^*$
4:1 pyrazole:Cu(II)	47 400	34300	$\pi \rightarrow \pi^* + n(\text{Pz}) \rightarrow \text{Cu(II)}$
	32 100	430	$\pi_1(\text{Pz}) \rightarrow \text{Cu(II)} + \pi_2(\text{Pz}) \rightarrow \text{Cu(II)}$
	13 900	41	LF
20:1 pyrazole:Cu(II)	33 200	740	$\pi_1(\text{Pz}) \rightarrow \text{Cu(II)} + \pi_2(\text{Pz}) \rightarrow \text{Cu(II)}$
	15 400	51	LF
3,5-dimethylpyrazole	46 700	5700	$\pi \rightarrow \pi^*$
4:1 3,5-dimethylpyrazole:Cu(II)	45 900	41200	$\pi \rightarrow \pi^* + n(\text{Pz}) \rightarrow \text{Cu(II)}$
	32 300	890	$\pi_2(\text{Pz}) \rightarrow \text{Cu(II)}$
	28 600	685	$\pi_1(\text{Pz}) \rightarrow \text{Cu(II)}$
	14 100	40	LF
20:1 3,5-dimethylpyrazole:Cu(II)	32 200	1490	$\pi_2(\text{Pz}) \rightarrow \text{Cu(II)}$
	28 300	1570	$\pi_1(\text{Pz}) \rightarrow \text{Cu(II)}$
	15 900	73	LF

<sup>a, b</sup> See footnotes for Table II.

**Figure 2.** Qualitative MO picture of the LMCT absorptions expected for Cu(II) complexes of ImH and Pz.

both types of complexes. From the above discussion, the lowest energy LMCT absorption in Cu(II)-ImH complexes unambiguously should be the  $\pi_1(\text{ImH}) \rightarrow \text{Cu(II)}$  transition. Detailed assignment of the lowest energy LMCT absorption in Cu(II)-Pz complexes is slightly less certain because the  $\pi_1$ - $\pi_2$  separation in the free ligand is smaller and  $\pi_1$  (the HOMO) should be more stabilized by complex formation than  $\pi_2$  (vide supra). However, the preferential stabilization of  $\pi_1$  must be more than  $\sim 0.7$  eV to induce a reversal of the level ordering, and it seems reasonable to assume that the  $\pi_1$  orbital remains the HOMO for complexed Pz as well, and hence that the lowest energy LMCT band in such complexes is the  $\pi_1(\text{Pz}) \rightarrow \text{Cu(II)}$  transition.

**1. Cu(II)-ImH.** The ligand  $\pi \rightarrow \pi^*$  absorption at 48 800 cm<sup>-1</sup> and  $n(\text{ImH}) \rightarrow \text{Cu(II)}$  LMCT absorption at 45 500 cm<sup>-1</sup> are well resolved in polycrystalline Cu(ImH)<sub>4</sub>SO<sub>4</sub>.<sup>1</sup> Moreover, splittings of the  $\pi_2(\text{ImH}) \rightarrow \text{Cu(II)}$  (41 700, 38 500 cm<sup>-1</sup>) and  $\pi_1(\text{ImH}) \rightarrow \text{Cu(II)}$  (32 800, 29 900 cm<sup>-1</sup>) absorptions occur in the spectra of polycrystalline samples and may be attributed to the two different orientations of ImH revealed by crystallographic studies. The  $\pi \rightarrow \pi^*$  ligand absorption and  $n(\text{ImH}) \rightarrow \text{Cu(II)}$  absorption appear as a single unresolved band at 48 800 cm<sup>-1</sup> ( $\epsilon$  41 000/mol of Cu) in the methanolic solution spectra of Cu(ImH)<sub>4</sub><sup>2+</sup> (Table II). Some contribution of  $n(\text{ImH}) \rightarrow \text{Cu(II)}$  LMCT to this absorption is indicated by the observed  $\epsilon$  being greater than the approximate value expected for the  $\pi \rightarrow \pi^*$  absorption alone ( $\epsilon \sim 28 000$ ). The shoulder at 32 300 cm<sup>-1</sup> ( $\epsilon \sim 350$ ) is the only feature in the solution spectra which can be associated with the  $\pi(\text{ImH}) \rightarrow \text{Cu(II)}$  absorptions exhibited by polycrystalline Cu(ImH)<sub>4</sub>SO<sub>4</sub>. We show below that separate and relatively intense  $\pi_1(\text{ligand}) \rightarrow \text{Cu(II)}$  and  $\pi_2(\text{ligand}) \rightarrow \text{Cu(II)}$  LMCT bands are exhibited by tetrakis Cu(II) complexes of substituted imidazole and pyrazole ligands. In contrast to the results for polycrystalline Cu(ImH)<sub>4</sub>SO<sub>4</sub>, splitting of the individual  $\pi$ -symmetry LMCT

(14) Noyce, D. S.; Ryder, E., Jr.; Walker, B. H. *J. Org. Chem.* **1955**, *20*, 1681-1686.

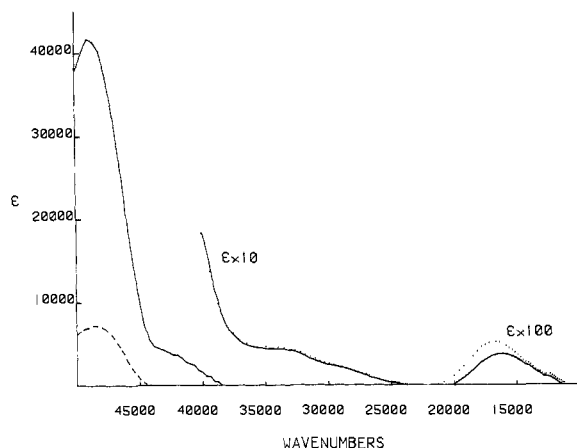


**Figure 3.** Electronic spectra at 25 °C of methanol solutions 0.0035 M in  $\text{Cu}(\text{ClO}_4)_2 \cdot 6\text{H}_2\text{O}$  and either 0.014 M (—) or 0.028 M (⋯) in ImH. Reference spectra of free ImH (0.014 M) are indicated by the broken line (---).

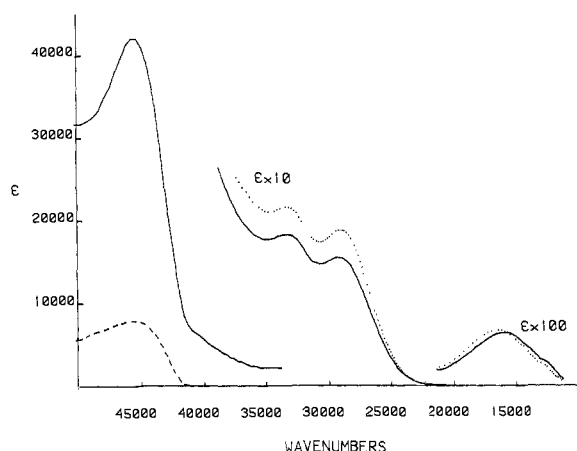


**Figure 4.** Electronic spectra at 25 °C of methanol solutions 0.0035 M in  $\text{Cu}(\text{ClO}_4)_2 \cdot 6\text{H}_2\text{O}$  and either 0.014 M (—) or 0.028 M (⋯) in 4,5-diethylimidazole. Reference spectra of the free ligand (0.014 M) are indicated by the broken line (---).

bands was not observed in the spectra of the solution complexes. Due to the relative broadness of the charge-transfer bands of solution species, nonequivalence of the ligands in these tetrakis complexes probably cannot be detected by electronic spectral techniques. Our spectroscopic results (Table II and Figure 3) indicate that the formation of  $\text{Cu}(\text{ImH})_4^{2+}$  is fairly complete when the ligand to Cu(II) ratio is 4:1 (the Cu(II) concentration is 0.0035 M) and effectively 100% when this ratio is increased to 8:1. In particular, the energy and intensity of the Cu(II) LF band at  $\sim 16\,100\text{ cm}^{-1}$  do not change significantly when the ligand to Cu(II) ratio is increased further. Assuming the formation constants of this system in methanol approximate those reported for aqueous solution,<sup>15a</sup> we estimate that >90% of the Cu(II) is present as the  $\text{Cu}(\text{ImH})_4^{2+}$  complex. In view of the similar behavior of the LF bands observed for the Cu(II)-4,5-dialkylimidazole systems, the dominant solution species also are the tetrakis complexes. The Cu(II)-ligand formation constants are not reduced seriously by ligand alkylation.<sup>15a</sup> Presumably the nonbonded interactions between the ligands are minimal because the imidazole rings and the  $\text{CuN}_4$  plane need not be coplanar.<sup>1</sup>

**2. Cu(II)-4,5-Disubstituted Imidazoles.** Substitution of ImH in the 4 and 5 positions yields Cu(II) complexes whose solution spectra display  $\pi(\text{ImH}) \rightarrow \text{Cu}(\text{II})$  LMCT absorptions which are considerably more intense and better resolved than those observed for  $\text{Cu}(\text{ImH})_4^{2+}$ . Electronic spectra of the Cu(4,5-diethyl-

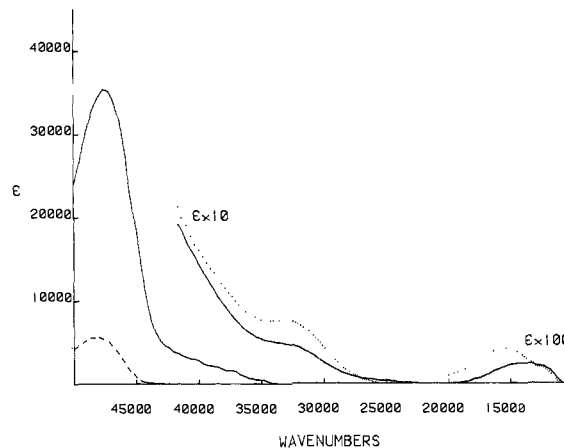


**Figure 5.** Electronic spectra at 25 °C of methanol solutions 0.0035 M in  $\text{Cu}(\text{ClO}_4)_2 \cdot 6\text{H}_2\text{O}$  and either 0.014 M (—) or 0.07 M (⋯) in Pz. Reference spectra of the free Pz are indicated by the broken line (---).

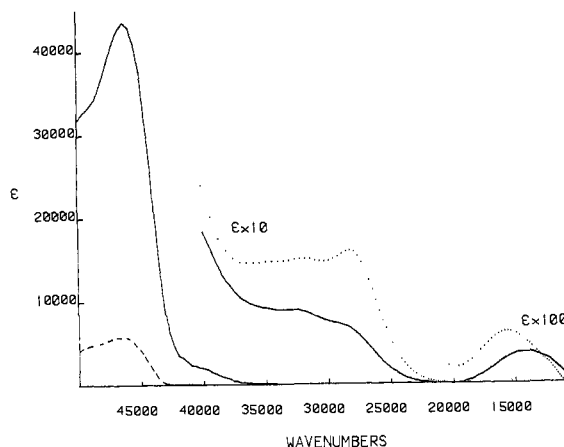


**Figure 6.** Electronic spectra at 25 °C of methanol solution 0.0035 M in  $\text{Cu}(\text{ClO}_4)_2 \cdot 6\text{H}_2\text{O}$  and either 0.014 M (—) or 0.07 M (⋯) in 3,5-dimethylpyrazole. Reference spectra of the free ligand are given by the broken line (---).

imidazole) $_4^{2+}$  complex are presented in Figure 4 and summarized in Table II. As above, complex formation is fairly complete when the ligand:Cu(II) ratio is 4:1 and essentially total when the ratio is increased to 8:1. Dialkylation has caused the unresolved  $\pi \rightarrow \pi^*$  ligand and  $n(\text{ligand}) \rightarrow \text{Cu}(\text{II})$  LMCT absorptions to be red-shifted to  $45\,200\text{ cm}^{-1}$ ; neither the intensity nor the position of the Cu(II) ligand field (LF) transitions significantly change. However, both the  $\pi_2(\text{ligand}) \rightarrow \text{Cu}(\text{II})$  and  $\pi_1(\text{ligand}) \rightarrow \text{Cu}(\text{II})$  LMCT absorptions are retained as prominent solution spectral features at  $33\,100\text{ cm}^{-1}$  ( $\epsilon\ 2110$ ) and  $28\,700\text{ cm}^{-1}$  ( $\epsilon\ 1830$ ), respectively. Similar results have been obtained for the Cu(II) complexes of 4,5-diisopropylimidazole, 4,5,6,7-tetrahydrobenzimidazole, and (+)-5-methyl-4,5,6,7-tetrahydrobenzimidazole, and they are summarized in Table II.

**3. Cu(II)-Pz.** Comparisons of the electronic spectra of free Pz and  $\text{Cu}(\text{Pz})_4^{2+}$  are presented as Figure 5 and Table III. Pyrazoles are considerably poorer ligands than imidazoles.<sup>15b</sup> As a result, the purification of pyrazoles is relatively easy. In addition, pyrazole:Cu(II) ratios of 20:1 were required to convert essentially all of the Cu(II) to the  $\text{Cu}(\text{ligand})_4^{2+}$  solution complex. Except for features reflecting these differences in formation constants, the solution spectra of  $\text{Cu}(\text{Pz})_4^{2+}$  are completely analogous to those described above for  $\text{Cu}(\text{ImH})_4^{2+}$ . The  $\pi \rightarrow \pi^*$  Pz absorption and  $n(\text{Pz}) \rightarrow \text{Cu}(\text{II})$  LMCT absorption both contribute to the unresolved band at  $47\,400\text{ cm}^{-1}$  ( $\epsilon\ 34\,300$ ). The combined  $\pi(\text{Pz}) \rightarrow \text{Cu}(\text{II})$  LMCT transitions appear as a weak spectral feature at  $33\,200\text{ cm}^{-1}$  ( $\epsilon\ 740$ ), while the LF absorption appears at  $15\,400\text{ cm}^{-1}$  ( $\epsilon\ 51$ ). The  $\pi$ -symmetry LMCT is slightly more pronounced than that observed for  $\text{Cu}(\text{ImH})_4^{2+}$  but becomes considerably more pronounced when the Pz is dialkylated (vide infra).

(15) (a) Nozaki, Y.; Gurd, F. R. N.; Chen, R. F.; Edsall, J. T. *J. Am. Chem. Soc.* **1957**, *79*, 2123-2129. (b) Sillen, L. G.; Martell, A. E. *Spec. Publ.-Chem. Soc.* **1971**, No. 25, 280-281, 369.

Table IV. Reassignment of Electronic Spectra Reported for Various Bis(1-pyrazolyl)borate M(II) and Bis(1-pyrazolyl)gallate M(II) Complexes

ref	complex	$\bar{\nu}$ , cm <sup>-1</sup>	$\epsilon$	assignment
16	Zn[H <sub>2</sub> B(Pz) <sub>2</sub> ] <sub>2</sub>	46 500 (sh) <sup>a</sup> 45 900 <sup>a</sup>	23000 24000	$\pi \rightarrow \pi^*$ ? $\pi \rightarrow \pi^*$
16	Cu[H <sub>2</sub> B(Pz) <sub>2</sub> ] <sub>2</sub>	49 300 <sup>a</sup> 45 700 <sup>a</sup> 37 700 <sup>b</sup> 30 500 <sup>b</sup> 18 500 <sup>b</sup>	20000 18000 1000 1000 68	$\pi \rightarrow \pi^* + n(\text{Pz}) \rightarrow \text{Cu(II)}$ $\pi_2(\text{Pz}) \rightarrow \text{Cu(II)}$ $\pi_1(\text{Pz}) \rightarrow \text{Cu(II)}$ LF
16	Co[H <sub>2</sub> B(Pz) <sub>2</sub> ] <sub>2</sub> <sup>c</sup>	48 100 <sup>a</sup> 41 300 <sup>a</sup> 35 700 <sup>a</sup>	18000 5000 1700	$\pi \rightarrow \pi^*$ $\pi_2(\text{Pz}) \rightarrow \text{Co(II)}$ $\pi_1(\text{Pz}) \rightarrow \text{Co(II)}$
17	Cu[Me <sub>2</sub> B(Pz) <sub>2</sub> ] <sub>2</sub>	31 600 <sup>a</sup> 20 000 <sup>a</sup> 17 000 (sh) <sup>a</sup>	1140 33 25	$\pi_1(\text{Pz}) \rightarrow \text{Cu(II)}$ LF LF
17	Cu[Me <sub>2</sub> Ga(Pz) <sub>2</sub> ] <sub>2</sub>	29 600 <sup>a</sup> 15 400 <sup>a</sup> 12 500 (sh) <sup>a</sup>	1190 93 66	$\pi_1(\text{Pz}) \rightarrow \text{Cu(II)}$ LF LF
17	Cu[Me <sub>2</sub> Ga(3,5-dimethyl-1-Pz) <sub>2</sub> ] <sub>2</sub>	37 700 <sup>a</sup> 24 700 <sup>a</sup> 20 200 <sup>a</sup> 12 000 (sh) <sup>a</sup> 9 380 <sup>a</sup>	2790 1900 1970 71 160	$n(\text{Pz}) \rightarrow \text{Cu(II)}$ $\pi_2(\text{Pz}) \rightarrow \text{Cu(II)}$ $\pi_1(\text{Pz}) \rightarrow \text{Cu(II)}$ LF LF

<sup>a</sup> Measured in cyclohexane. <sup>b</sup> Measured in CH<sub>2</sub>Cl<sub>2</sub>. <sup>c</sup> LF absorptions in the visible and infrared regions have not been included here.

**4. Cu(II)-3,5-Dimethylpyrazole.** Electronic spectra of this system are presented in Figure 6 and summarized in Table III. Alkylation of Pz in the 3 and 5 positions causes the ligand  $\pi \rightarrow \pi^*$  absorption to red shift to 46 700 cm<sup>-1</sup> ( $\epsilon$  5700). The mixed ligand  $\pi \rightarrow \pi^*$  absorption and  $n(\text{ligand}) \rightarrow \text{Cu(II)}$  LMCT band appear as a broad unresolved band at 45 900 cm<sup>-1</sup> ( $\epsilon$  41 200) in the complex. Formation of the Cu(ligand)<sub>4</sub><sup>2+</sup> complex appears to be complete at a 20:1 ligand:Cu(II) ratio. The LF band occurs at 15 900 cm<sup>-1</sup> ( $\epsilon$  73) and prominent resolved  $\pi_2(\text{ligand}) \rightarrow \text{Cu(II)}$  and  $\pi_1(\text{ligand}) \rightarrow \text{Cu(II)}$  LMCT absorptions appear at 32 200 cm<sup>-1</sup> ( $\epsilon$  1490) and 28 300 cm<sup>-1</sup> ( $\epsilon$  1570), respectively.

**5. Planar and Tetrahedral (1-Pyrazolyl)<sub>2</sub>X-M<sup>II</sup> Complexes,** X = H<sub>2</sub>B, Me<sub>2</sub>B, Me<sub>2</sub>Ga and M<sup>II</sup> = Cu<sup>II</sup>, Zn<sup>II</sup>, Co<sup>II</sup>. Having elucidated the electronic spectra of Cu(Pz)<sub>4</sub><sup>2+</sup> units, it is worthwhile to reconsider the published electronic spectra of Cu(II) (and other divalent transition-metal ions) complexed to polydentate pyrazole ligands. The preparation and study of poly(1-pyrazolyl)borate ligands was initiated by Trofimenko and co-workers.<sup>16</sup> Of particular interest are complexes of the bis(1-pyrazolyl)borate ligand H<sub>2</sub>B(Pz)<sub>2</sub><sup>-</sup>; complexes of the closely related bis(1-pyrazolyl)dimethylgallate ligands Me<sub>2</sub>Ga(Pz)<sub>2</sub><sup>-</sup> have been characterized by Storr and co-workers.<sup>17,18</sup> Selected published electronic spectra<sup>16,17</sup> are summarized in Table IV. The presumably tetrahedral Zn[H<sub>2</sub>B(Pz)<sub>2</sub>]<sub>2</sub> complex is spectroscopically transparent except for the ligand  $\pi \rightarrow \pi^*$  band at 45 900 cm<sup>-1</sup> ( $\epsilon$  24 000) accompanied by a shoulder at 46 500 cm<sup>-1</sup> ( $\epsilon$  23 000). The reduced intensity of this band relative to those observed for Cu(Pz)<sub>4</sub><sup>2+</sup> analogues (Table III) may be attributed to the absence of an approximately energetically degenerate  $n(\text{Pz}) \rightarrow \text{M(II)}$  LMCT absorption.

The structural constraints of this chelating ligand apparently are as effective as dialkylation in preserving the solution spectral features of  $\pi(\text{ligand}) \rightarrow \text{Cu(II)}$  LMCT transitions. The Cu-[H<sub>2</sub>B(Pz)<sub>2</sub>]<sub>2</sub> complex should possess an approximately planar CuN<sub>4</sub> unit in view of the LF absorption at 18 500 cm<sup>-1</sup> ( $\epsilon$  68). Absorptions at 45 700 cm<sup>-1</sup> ( $\epsilon$  18 000) and 49 300 cm<sup>-1</sup> ( $\epsilon$  30 000) are appropriate in energy and intensity for ligand  $\pi \rightarrow \pi^*$  and  $n(\text{ligand}) \rightarrow \text{Cu(II)}$  LMCT absorptions. Additional absorptions at 37 700 cm<sup>-1</sup> ( $\epsilon$  1000) and 30 500 cm<sup>-1</sup> ( $\epsilon$  1000) reasonably may be assigned to  $\pi_2(\text{ligand}) \rightarrow \text{Cu(II)}$  and  $\pi_1(\text{ligand}) \rightarrow \text{Cu(II)}$  LMCT bands, respectively. The original assignment of these latter

two absorptions as LF bands certainly is incorrect. The corresponding Co[H<sub>2</sub>B(Pz)<sub>2</sub>]<sub>2</sub> complex exhibits characteristic visible and near-IR spectra (not included in Table IV) of a tetrahedral Co(II) species. The absorption at 48 100 cm<sup>-1</sup> ( $\epsilon$  18 000) is attributable to the expected ligand  $\pi \rightarrow \pi^*$  absorption. The expected  $n(\text{ligand}) \rightarrow \text{Co(II)}$  LMCT band should be well removed toward higher energy due to the relatively poor oxidizing ability of Co(II). However, the expected  $\pi_2(\text{ligand}) \rightarrow \text{Co(II)}$  and  $\pi_1(\text{ligand}) \rightarrow \text{Co(II)}$  LMCT transitions no doubt correspond to the absorptions at 41 300 ( $\epsilon$  5000) and 35 700 cm<sup>-1</sup> ( $\epsilon$  1700). The strength of the former absorption may reflect intensity borrowing from the neighboring ligand  $\pi \rightarrow \pi^*$  absorption. Due to a combination of redox and LF effects  $\pi(\text{ligand}) \rightarrow \text{Co(II)}$  LMCT absorptions are blue shifted approximately 3000–4000 cm<sup>-1</sup> relative to corresponding absorptions of the planar Cu(II) analogue.

The Cu[Me<sub>2</sub>B(Pz)<sub>2</sub>]<sub>2</sub> complex characterized by Storr and co-workers<sup>17</sup> appears entirely analogous to the Cu[H<sub>2</sub>B(Pz)<sub>2</sub>]<sub>2</sub> complex described above. Absorptions at 20 000 cm<sup>-1</sup> ( $\epsilon$  33) and 17 000 cm<sup>-1</sup> (sh,  $\epsilon$  25) clearly are LF in character. A higher energy band at 31 600 cm<sup>-1</sup> ( $\epsilon$  1140), previously unassigned, reasonably may be attributed to  $\pi_1(\text{Pz}) \rightarrow \text{Cu(II)}$  LMCT absorption. A full X-ray crystallographic characterization<sup>18</sup> has been reported for Cu-[Me<sub>2</sub>Ga(Pz)<sub>2</sub>]<sub>2</sub>, which contains a planar CuN<sub>4</sub> chromophore. Absorptions at 15 400 ( $\epsilon$  93) and 12 500 cm<sup>-1</sup> (sh,  $\epsilon$  66) have been assigned as LF transitions. A higher energy band at 29 600 cm<sup>-1</sup> ( $\epsilon$  1190), not previously assigned, may be attributed to  $\pi_1(\text{Pz}) \rightarrow \text{Cu(II)}$  LMCT absorption; reflectance measurements disclosed a similar absorption at 25 000 cm<sup>-1</sup> for the polycrystalline complex. We next consider Cu[Me<sub>2</sub>Ga(3,5-Me<sub>2</sub>Pz)<sub>2</sub>]<sub>2</sub> which also has been fully characterized by X-ray crystallography<sup>18</sup> as well as other studies.<sup>17</sup> Alkylation of the pyrazole units causes the CuN<sub>4</sub> donor set to adopt a nearly tetrahedral geometry. The dihedral angle between two of the N–Cu–N units is 71.9° (90° for an idealized tetrahedral geometry). Convincing evidence has been presented that this geometry also is maintained in cyclohexane solutions of the complex.<sup>17</sup> The reflectance spectra of the polycrystalline complex are similar to the solution spectra. Moreover, the A<sub>11</sub> Cu hyperfine splitting is less than half that observed for the planar Cu[Me<sub>2</sub>Ga(Pz)<sub>2</sub>]<sub>2</sub> complex. Solution spectra of the above pseudotetrahedral chromophore includes absorptions at 12 000 (sh,  $\epsilon$  71) and 9380 cm<sup>-1</sup> ( $\epsilon$  160), which reasonably were assigned to LF transitions. Higher energy absorptions at 37 700 ( $\epsilon$  2790), 24 690 ( $\epsilon$  1900), and 20 200 cm<sup>-1</sup> ( $\epsilon$  1970) now may be assigned as  $n(\text{Pz}) \rightarrow \pi_2(\text{Pz}) \rightarrow$ , and  $\pi_1(\text{Pz}) \rightarrow \text{Cu(II)}$  LMCT transitions, respectively. All three absorptions are substantially red shifted from the corresponding absorptions observed for approximately planar Cu(Pz)<sub>4</sub><sup>2+</sup> species.

(16) Jesson, J. P.; Trofimenko, S.; Eaton, D. R. *J. Am. Chem. Soc.* **1967**, *89*, 3148–3158.

(17) Herring, F. G.; Patmore, D. J.; Storr, A. *J. Chem. Soc., Dalton Trans.* **1975**, 711–717.

(18) Patmore, D. J.; Rendle, D. F.; Storr, A.; Trotter, J. *J. Chem. Soc., Dalton Trans.* **1975**, 718–725.

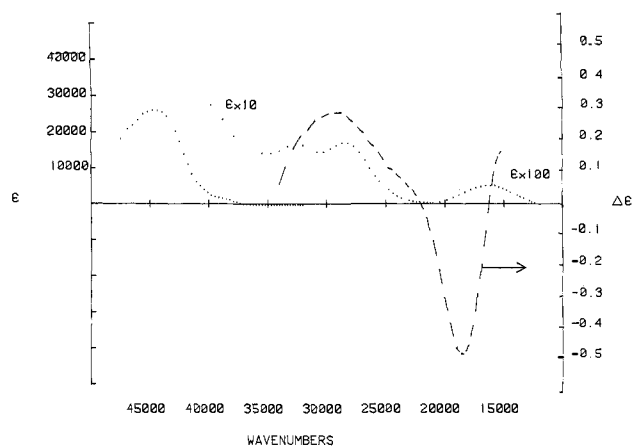


**Figure 7.** Circular dichroism spectra at 25 °C of methanol solutions 0.001 M in  $\text{Cu}(\text{ClO}_4)_2 \cdot 6\text{H}_2\text{O}$  and 0.004 M in (+)-5-methyl-4,5,6,7-tetrahydrobenzimidazole (---); electronic spectra at 25 °C of methanol solutions 0.0035 M in  $\text{Cu}(\text{ClO}_4)_2 \cdot 6\text{H}_2\text{O}$  and 0.014 M in ligand.

**6. CD Spectra of Cu(II)-(+)5-Methyl-4,5,6,7-tetrahydrobenzimidazole.** The circular dichroism (CD) and electronic spectra of this system are presented in Figure 7. Our original goal was to compare the Kuhn anisotropy factors ( $\gamma = |\Delta\epsilon/\epsilon|$ ) of the  $\sigma$ - and  $\pi$ -symmetry LMCT absorptions. Other workers have measured the Kuhn factors of type I copper protein absorptions and used these results to facilitate the assignment of the LMCT transitions.<sup>19</sup> We are unable to compare the Kuhn factors of the  $n(\text{ligand}) \rightarrow \text{Cu}(\text{II})$  and  $\pi(\text{ligand}) \rightarrow \text{Cu}(\text{II})$  absorptions, because the former and the ligand  $\pi \rightarrow \pi^*$  absorptions could not be resolved in either the CD or electronic spectra. Although the  $\pi_2(\text{ligand}) \rightarrow$  and  $\pi_1(\text{ligand}) \rightarrow \text{Cu}(\text{II})$  LMCT absorptions were particularly well resolved in the solution spectra, their resolution in the CD spectra (Figure 1) is poor. The  $\Delta\epsilon$  and Kuhn factor for the  $\pi_2(\text{ligand}) \rightarrow \text{Cu}(\text{II})$  band at 32 300  $\text{cm}^{-1}$  are 0.30 and 0.00016, respectively, whereas the corresponding values for the  $\pi_1(\text{ligand}) \rightarrow \text{Cu}(\text{II})$  band at 28 600  $\text{cm}^{-1}$  are 0.24 and 0.00012, respectively. The  $\Delta\epsilon$  and Kuhn factor for the LF band at 17 500  $\text{cm}^{-1}$  are -0.25 and 0.0034, respectively. The copper protein spectra have been assigned by using a scheme in which the Kuhn factors of LF,  $\sigma$ -symmetry LMCT, and  $\pi$ -symmetry LMCT absorptions span the respective ranges of 0.0005–0.0045, 0.0029–0.015, and 0.00034–0.0017. The results from our model complex strongly suggest that for simple systems, the Kuhn factors of  $\pi$ -symmetry LMCT bands can be smaller than those of probably analogous copper protein absorptions. The significance of this result is not clear. We are concerned that the  $\Delta\epsilon$  in the copper protein absorptions is induced both by the chirality of the local peptide ligation and the chirality of the helical protein structure. This latter effect has of course not been accounted for in our model.

### Conclusions and Applications to Cu(II)-Protein Spectra.

In the preliminary account<sup>1</sup> of  $\text{ImH} \rightarrow \text{Cu}(\text{II})$  LMCT absorptions, we noted possible applications of these results to tetragonal Cu(II) protein chromophores, which included ligation by several histidine-imidazole groups. A number of significant spectroscopic findings have resulted from the extension of our work as reported here. First, prominent near UV  $\pi(\text{ImH}) \rightarrow \text{Cu}(\text{II})$  LMCT absorptions have been identified in the solution spectra of Cu(II) complexed to substituted imidazoles. Presumably unsubstituted ImH can adopt a continuum of conformations relative to the  $\text{CuN}_4$  unit in  $\text{Cu}(\text{ImH})_4^{2+}$  complexes. This effect serves

to severely broaden the  $\pi(\text{ImH}) \rightarrow \text{Cu}(\text{II})$  LMCT bands. Secondly, the electronic spectral structures of pyrazole and imidazole are strikingly similar. Both  $\text{Cu}(\text{ImH})_4^{2+}$  and  $\text{Cu}(\text{Pz})_4^{2+}$  exhibit poorly resolved  $\pi(\text{ligand}) \rightarrow \text{Cu}(\text{II})$  LMCT absorptions at nearly the same energies. Alkylation of the rings transforms the  $\pi(\text{ligand}) \rightarrow \text{Cu}(\text{II})$  LMCT absorptions to fairly intense well-resolved spectral features. Cu(II) complexes of substituted imidazoles and pyrazoles exhibit these absorptions at comparable energies and with comparable intensities. These results allow us to reliably interpret the electronic spectra reported for a pseudotetrahedral  $\text{Cu}(\text{Pz})_4^{2+}$  chromophore fully characterized by Storr and co-workers.<sup>17,18</sup> The data in Table IV support our previous estimate<sup>1</sup> that LMCT absorptions undergo an approximately 10 000–12 000- $\text{cm}^{-1}$  red shift when typical Cu(II) chromophores adopt a pseudotetrahedral geometry. Red shifts in this range are exhibited by all three  $\text{Pz} \rightarrow \text{Cu}(\text{II})$  LMCT absorptions. Another point of interest is that due to the different redox properties of Co(II) and Cu(II), the  $\pi_2(\text{Pz}) \rightarrow \text{Co}(\text{II})$  and  $\pi_1(\text{Pz}) \rightarrow \text{Co}(\text{II})$  LMCT absorptions are blue shifted 16 600 and 15 500  $\text{cm}^{-1}$ , respectively, from the corresponding absorptions reported for the pseudotetrahedral Cu(II) analogue. Blue shifts in the range of 13 400–15 600  $\text{cm}^{-1}$  have been postulated for  $\text{S}(\text{thiolate}) \rightarrow \text{M}(\text{II})$  LMCT absorptions when Co(II) is substituted for Cu(II) in plastocyanin, azurin, and stellacyanin.<sup>19,20</sup> This interpretation of the metal substitution studies is supported by the results presented above as well as by our previous study of a model Co(II) thiolate complex.<sup>21</sup>

We now consider the application of our results to the electronic spectra reported for the type I copper proteins.<sup>2</sup> X-ray crystallographic studies at approximately 3 Å resolution of an azurin<sup>22</sup> and a plastocyanin<sup>23</sup> have revealed that both proteins contain distorted  $\text{CuN}_2\text{SS}^*$  units with ligation by two imidazoles (N), a thiolate sulfur (S) from cysteine, and a thioether sulfur ( $\text{S}^*$ ) from methionine. More recent studies of the plastocyanin at 1.6 Å resolution<sup>24</sup> have better defined the geometry of its  $\text{CuN}_2\text{SS}^*$  unit and have revealed that the thioether is apically bound ( $\text{Cu}-\text{S}^* \sim 2.9$  Å). These three proteins exhibit two or more absorptions in the 18 000–23 000- $\text{cm}^{-1}$  spectral range.<sup>2</sup> The absorptions of the model pseudotetrahedral  $\text{Cu}(\text{Pz})_4^{2+}$  unit at 24 700 and 20 200  $\text{cm}^{-1}$  (Table IV) have been assigned to  $\pi_2(\text{Pz}) \rightarrow$  and  $\pi_1(\text{Pz}) \rightarrow \text{Cu}(\text{II})$  LMCT absorptions, respectively, in this work. Corresponding absorptions in this visible-near-UV spectral range are expected for either equivalent or crystallographically different Cu(II)-imidazole bonding in the type I proteins. The possibility of observing LMCT in this spectral region from the apical thioether-Cu(II) bonding will be considered elsewhere.<sup>25</sup>

**Acknowledgment.** This work was supported by the National Institutes of Health (Grant AM-16412 to H.J.S.). We thank Professors S. Knapp and A. Hagedorn for helpful advice regarding the ligand syntheses.

(20) McMillin, D. R.; Rosenberg, R. C.; Gray, H. B. *Proc. Natl. Acad. Sci. U.S.A.* **1974**, *71*, 4760–4762.

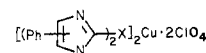
(21) Mastropaolo, D.; Thich, J. A.; Potenza, J. A.; Schugar, H. J. *J. Am. Chem. Soc.* **1977**, *99*, 424–429.

(22) Adman, E. T.; Stenkamp, R. E.; Sieker, L. C.; Jensen, L. H. *J. Mol. Biol.* **1978**, *123*, 35–47.

(23) Colman, P. M.; Freeman, H. C.; Guss, J. M.; Murata, M.; Norris, V. A.; Ramshaw, J. A. M.; Venkatappa, M. P. *Nature (London)* **1978**, *272*, 319–324.

(24) Private communication from Professor Hans Freeman.

(25) The complexes



where  $\text{X} = >\text{C}(\text{CH}_3)_2$ ,  $\text{CH}_2\text{SCH}_2$  have been spectroscopically and crystallographically characterized in our laboratory. The former complex has a planar  $\text{CuN}_4$  unit whereas the latter has a tetragonal  $\text{CuN}_4\text{S}_2^*$  unit with apical ligation by the thioether donors: Prochaska, H. J.; Schwindinger, W. F.; Schwartz, M.; Burk, M. J.; Bernarducci, E.; Lalancette, R. A.; Potenza, J. A.; Schugar, H. J., *J. Am. Chem. Soc.*, in press.

(19) Tennent, D. L.; McMillin, D. R. *J. Am. Chem. Soc.* **1979**, *101*, 2307–2311.